Original Article

STING facilitates the development of radiation-induced lung injury via regulating the PERK/eIF2α pathway

Xiangwei Ge[1,2#], Qiaowei Liu[3,4#], Hao Fan[1,2], Hongyang Yu[1], Jinfeng Li[3], Yao Li[1,2], Boyu Qin[3], Junxun Ma[3], Jinliang Wang[3], Yi Hu[2]

[1]Medical School of Chinese PLA, Beijing, China; [2]Department of Oncology, the First Medical Center, Chinese PLA General Hospital, Beijing, China; [3]Department of Oncology, the Fifth Medical Center, Chinese PLA General Hospital, Beijing, China; [4]Department of Emergency, the Fifth Medical Center, Chinese PLA General Hospital, Beijing, China

Contributions: (I) Conception and design: Y Hu, J Wang, X Ge, Q Liu; (II) Administrative support: Y Hu; (III) Provision of study materials or patients: J Ma; (IV) Collection and assembly of data: X Ge, Q Liu, H Fan, H Yu; (V) Data analysis and interpretation: X Ge, J Li, Y Li, B Qin; (VI) Manuscript writing: All authors; (VII) Final approval of manuscript: All authors.

[#]These authors contributed equally to this work.

Correspondence to: Yi Hu, MD, PhD. Department of Oncology, the First Medical Center, Chinese PLA General Hospital, 28 Fuxing Road, Haidian District, Beijing 100853, China. Email: huyi301zlxb@sina.com; Jinliang Wang, MD. Department of Oncology, the Fifth Medical Center, Chinese PLA General Hospital, 4th West Ring Road 100, Fengtai District, Beijing 100039, China. Email: wangjinliang301@163.com.

Background: Radiation-induced lung injury (RILI) is one of the serious adverse reactions of thoracic radiotherapy, which largely limits the dose and therapeutic effect of radiotherapy. The underlying mechanism has not been elucidated. RILI is characterized by an acute inflammatory response, and stimulator of interferon genes (STING) has been reported to play an important role in regulating inflammation and innate immune activation. However, its role in RLLI, remains unclear. Here, we reported the potential therapeutic effect of STING inhibitor H-151 on RILI.

Methods: C57BL/6J mice were exposed to 20 Gy whole-thorax irradiation and H-151 was injected intraperitoneally from the day of irradiation for 4 weeks. The degree of RILI was then assessed. To further explore the mechanism of STING in RILI, the supernatant of irradiated lung epithelial cell MLE-12 was co-cultured with embryonic fibroblast cell NIH/3T3.

Results: The cyclic guanosine monophosphate-adenosine monophosphate synthase (cGAS)-STING pathway is abnormally activated in irradiated mouse lung tissues. The early application of STING inhibitor significantly alleviated radiation-induced inflammatory cell infiltration and pro-inflammatory cytokine release in lung tissue, as well as the degree of fibrosis in the late stage. The amount of double-stranded DNA (dsDNA) in the supernatant of irradiated MLE-12 cells was abnormally increased, and the epithelial-derived dsDNA could promote the transformation of fibroblasts into myofibroblasts. Mechanistically, STING could mediate the activation of fibroblasts to myofibroblasts via the PKR-like endoplasmic reticulum kinase (PERK)-eukaryotic initiation factor 2α (eIF2α) pathway.

Conclusions: Our study focused on the activation of cGAS-STING signaling pathway in RILI, and inhibition of STING significantly ameliorated RILI in mice. STING mediated the effect of radiation-induced dsDNA release to stimulate the activation of inflammatory response, and STING restriction significantly delayed the fibrosis process through the PERK-eIF2α pathway, suggesting that STING intervention may pave a new avenue for the treatment of RILI.

Keywords: Radiation-induced lung injury (RILI); stimulator of interferon genes (STING); inflammation; fibrosis; PKR-like endoplasmic reticulum kinase (PERK)

Submitted Jul 24, 2024. Accepted for publication Oct 12, 2024. Published online Nov 21, 2024.
doi: 10.21037/tlcr-24-649
View this article at: https://dx.doi.org/10.21037/tlcr-24-649

Introduction

The incidence of malignant tumors has been increasing in recent years. As one of the main methods for the treatment of lung cancer, esophageal cancer, breast cancer, and other thoracic malignant tumors, radiotherapy plays an important role in the comprehensive treatment of malignant tumors (1-3). However, due to the inevitable damage to the surrounding normal tissues and the relative sensitivity of the lung to ionizing radiation, radiation-induced lung injury (RILI) occurs frequently (4,5). As a common serious complication of tumor radiotherapy, RILI mainly includes two stages: radiation pneumonitis (RP) in the early stage; and radiation-induced pulmonary fibrosis (RIPF) in the late stage (6,7). The occurrence of RILI will greatly affect the quality of life of patients, and also severely limit the dose and efficacy of radiotherapy (8). Currently, RILI is typically treated with high doses of corticosteroids to temporarily relieve symptoms. However, these treatments come with significant side effects, such as edema, sleep disturbances and weight gain, which may make corticosteroids inappropriate for the prevention of RILI or long-term use (4). Therefore, it is urgent to further explore its mechanism, identify more effective intervention targets, and develop new drugs to prevent RILI.

The lung is constantly exposed to the external environment, so it must have strong innate immunity to maintain host homeostasis. The innate immune response recognizes the pathogen-associated molecular pattern (PAMP) structure in pathogenic organisms through pattern recognition receptors, which in turn promotes the expression of type I interferons (IFNs) and other cytokines (9). As an important signaling pathway of innate immunity, the cyclic guanosine monophosphate-adenosine monophosphate synthase (cGAS)-stimulator of IFN genes (STING) pathway induces the expression of inflammatory molecules, which plays an important role in anti-infection immunity and systemic inflammatory response (10,11). It has been shown that DNA can also act as PAMPs in the case of damage (12). Cytosolic free double-stranded DNA (dsDNA) can bind to cGAS and catalyse synthesis of cyclic guanosine monophosphate-adenosine monophosphate (cGAMP) to activate STING protein. Then, TANK-binding kinase 1 (TBK1) mediates the nuclear translocation of IFN regulatory factor 3 (IRF3) to induce type I IFNs expression, and nuclear factor kappa-B (NF-κB) induces IFN-β, IL-6 and TNF-α expression (9,13-15). Hu *et al.* found that STING inhibitor could effectively improve myocardial inflammation (16), which suggests that STING, as an important adaptor protein regulating type I IFN gene expression, has potential value in the treatment of inflammation. These studies provide a theoretical basis for the application of STING inhibitors in radiation pneumonia.

Ionizing radiation is capable of inducing cell death and leads to the release of dsDNA into the cytoplasm or extracellular. Du *et al.* (17) found that dsDNA accumulates in the interstitial space of liver tissue in large numbers after radiotherapy, and dsDNA can further activate the cGAS-STING-IFN signaling axis of immune cells to induce hepatocyte necrosis, which is a key pathway of radiation-induced liver injury. However, the role of STING in RILI, especially in RIPF, has not been reported. Independent of activation of the TBK1-IRF3 pathway, the non-canonical pathway is primarily regulated by PKR-like endoplasmic

Highlight box

Key findings

- Stimulator of interferon genes (STING) mediates the effect of radiation-induced double-stranded DNA (dsDNA) release to stimulate the activation of the inflammatory response, and STING restriction significantly delays the fibrosis process through the PKR-like endoplasmic reticulum kinase (PERK)-eukaryotic initiation factor 2α (eIF2α) pathway. Based on the above mechanism, STING inhibitor H-151 could significantly alleviate radiation-induced lung injury (RILI).

What is known and what is new?

- The mechanism of RILI is complex and there is no effective treatment. RILI is characterized by inflammation in the early stage and fibrosis in the late stage. STING, as a popular research target in recent years, is known to play an important role in anti-infection immunity and systemic inflammatory response.
- Our study innovatively focuses on the activation of cyclic guanosine monophosphate-adenosine monophosphate synthase (cGAS)-STING signaling pathway in RILI, and STING inhibition significantly ameliorated RILI in mice. On the one hand, we creatively found that STING mediates the effect of radiation-induced dsDNA release to stimulate the activation of inflammatory response. On the other hand, dsDNA released from irradiated lung epithelial cells could activate the transformation of fibroblasts into myofibroblasts, and STING restriction significantly delayed the fibrosis process through PERK-eIF2α pathway. As we know, this is the first study of the STING-PERK-eIF2α pathway in RILI.

What is the implication, and what should change now?

- The study demonstrated the protective effect of STING inhibitor on RILI. Our results provided new insights into the molecular pathogenesis of radiation injury, and elucidating the PERK-eIF2α pathway may be able to guide future pharmacological interventions.

reticulum kinase (PERK) and eukaryotic initiation factor 2α (eIF2α) (18). Activated STING directly stimulates PERK to phosphorylate eIF2α, which is physiologically essential for cellular senescence and organ fibrosis (18). Intervention in the non-canonical STING-PERK-eIF2α pathway alleviates lung and kidney fibrosis, which provides a new direction for the treatment of RILI. Based on the above studies, we hypothesized that lung epithelial cell damage after radiotherapy generates a large amount of ectopic dsDNA, which can activate the transformation of fibroblasts into myofibroblasts by activating STING-PERK-eIF2α pathway, and STING restriction may effectively prevent this process.

To investigate this hypothesis, we designed a mouse model of RILI in which mice received 20 Gy whole-thorax irradiation (19). H-151, a potent and selective small molecule antagonist of STING (20), was administered by intraperitoneal injection at a dose of 10.5 mg/kg for 4 weeks starting on the day of irradiation. Our findings suggested that the cGAS-STING pathway was abnormally activated in irradiated mouse lung tissues. H-151 significantly reduced the release of proinflammatory cytokines and inflammatory infiltration in the process of RP, as well as collagen deposition in the process of RIPF, thereby delaying the progression of RILI. By irradiating lung epithelial cell line MLE-12, we found that irradiated epithelial-derived dsDNA stimulated fibroblast-to-myofibroblast transformation by activating the STING-PERK-eIF2α pathway, while knockdown of STING significantly inhibited the fibroblast transformation process. These results provided new insights into the molecular pathogenesis of radiation injury and elucidated that the STING-PERK-eIF2α pathway may be able to guide future pharmacological interventions. We present this article in accordance with the ARRIVE reporting checklist (available at https://tlcr.amegroups.com/article/view/10.21037/tlcr-24-649/rc).

Methods

Reagents and antibodies

STING inhibitor H-151(Cat # HY-112693) and PERK activator CCT020312 (Cat # HY-119240) were purchased from MedChemExpress (Monmouth Junction, USA); Anti-cGAS (Cat # 79978), anti-STING (Cat # 13647), anti-TBK1 (Cat # 38066), anti-p-TBK1 (Cat # 5483), anti-PERK (Cat # 3192), anti-p-PERK (Cat # 3179), anti-eIF2α (Cat # 5324), anti-p-eIF2α (Cat # 3398), anti-α-Tubulin (Cat # 3873), and anti-α-SMA (Cat # 19245) were purchased from Cell Signaling Technology (Danvers, USA). Anti-P16 (Cat # sc-1661) and anti-P21 (Cat # sc-6246) were purchased from Santa Cruz Biotechnology (Texas, USA). Masson Staining Kit (Cat # G1340) was purchased from Solarbio (Beijing, China). Senescence β-galactosidase staining kit (Cat # C0602) was purchased from Beyotime (Shanghai, China). Enzyme-linked immunosorbent assay (ELISA) kits for TNF-α, IL-1β, and IL-6 (Cat # MTA00B, MLB00C, M6000B) were purchased from R&D Systems (Minneapolis, USA). Lipofectamine RNAiMAX (Cat # 13778030) was purchased from Thermo Fisher Scientific (Waltham, USA). Poly(dA:dT) (Cat # tlrl-patc) was purchased from InvivoGen (San Diego, CA, USA). Dnase I (Cat # EN401) was purchased from Vazyme (Nanjing, China).

In vivo experiment

Male C57BL/6J mice (6–8 weeks old, 19–21 g) were purchased from SPF (Beijing) biotechnology. Mice were kept under controlled conditions (40% to 70% relative humidity, 24±2 ℃, 12-hour light /12-hour dark cycle) and given standard laboratory water and diet. The study includes two parts of animal experiments. Mice in the first stage were randomly divided into four groups: the control group, 12 hours after irradiation, 24 hours after irradiation, and 48 hours after irradiation (n=6 per group). In the second part of animal experiments, mice were randomly divided into three groups before irradiation, including the control group, the irradiation group, and the irradiation plus administration group (n=30 per group), and the time points of sample collection were 1, 2, 4, 12 and 24 weeks, respectively. For irradiation, the mice were anesthetized by intraperitoneal injection of pentobarbital sodium (50 mg/kg) and then placed in a special box that fully exposed their chests and kept their chests at the same level. Thick lead plates were carefully positioned to cover all areas of the mouse except for the chest. A single dose of 20 Gy whole-thorax X-ray radiation was performed on mice with the RS2000 Biological Irradiator (irradiation dose: 1.325 Gy/min). For the drug administration, mice were intraperitoneally injected with H-151 (10.5 mg/kg) once a day for the 4 consecutive weeks from the day of irradiation. The mice were euthanized at the corresponding time points and the samples were collected. The experiments were performed under a project license (No. IACUC-DWZX-2022-864) approved by the Institutional Animal

Care and Use Committee of the Beijing Institute of Radiation Medicine, in compliance with the Chinese national or institutional guidelines for the care and use of animals. The protocol was prepared before the study but not registered.

Sample collection

Mice were euthanized at corresponding time points after irradiation, and subsequently blood was collected and left at room temperature for 1 hour. After centrifugation at 3,000 rpm for 15 min, serum from the upper layer of the centrifuge tube was collected and stored at −80 ℃. Bronchoalveolar lavage fluid (BALF) was collected from mice at time points 12, 24 and 48 hours after irradiation. The trachea was exposed after mice were sacrificed, and a puncture needle was inserted into the trachea. Then, BALF was collected by lavage three times with 0.8 mL phosphate-buffered saline (PBS), and the supernatant was collected after centrifugation and stored at −80 ℃. Collected serum and BALF were used for ELISA and determination of dsDNA content. The lung tissues were separated into several parts. Some of them were stored at −80 ℃ and then used for molecular experiments such as western blot. Other tissues were temporarily preserved in paraformaldehyde for subsequent histopathological analysis.

ELISA analysis

TNF-α, IL-1β, and IL-6 levels in serum were determined by ELISA kits according to the manufacturer's instructions by R&D Systems (Minneapolis, USA). The optical density values of each well at 450 nm were examined within 30 min.

Histological analysis

The lung tissue was fixed in 4% paraformaldehyde for 24 hours. The tissues were then dehydrated and embedded with paraffin. Paraffin tissues were cut into sections with a thickness of 4 μm and stored at room temperature for subsequent experiments. For hematoxylin and eosin (H&E) staining, the tissue sections were stained with hematoxylin and eosin, and then were scored after staining. The scoring system included the width of alveolar septum, the degree of fibrosis exudation, and the degree of inflammatory cell infiltration. Each item is composed of 0–4 points, and the sum of the three items is the total score. For Masson staining, experiment was performed according to the manufacturer's instructions by Solarbio (Beijing, China). ImageJ software was used to calculate the positive areas of collagen.

Immunohistochemistry

After deparaffinized, the sections were taken for antigen retrieve. Next, these sections were incubated in 3% H_2O_2 for 15 min at room temperature to block endogenous peroxidase, followed by blocking with goat serum at room temperature for 30 min. The sections were incubated with anti-α-SMA or anti-COL1A1 antibody overnight at 4 ℃ and then incubated with the corresponding secondary antibody working solution for 30 min at room temperature. The slides were sealed after color development using DAB kit.

Cell culture

Murine lung epithelial-12 (MLE-12) and mouse embryonic fibroblast cells (NIH/3T3) were purchased from American Type Culture Collection. NIH/3T3 was cultured in Dulbecco's Modified Eagle Medium (DMEM) (Gibco, San Diego, USA) supplemented with 10% newborn calf serum (NCS) (Gibco). MLE-12 was cultured in DMEM/F12 supplemented with 2% fetal bovine serum (FBS) (Gibco). The cells were cultured at 37 ℃ in an atmosphere with 5% CO_2. For irradiation, RS2000 biological irradiator was used to irradiate cells with a single dose of 10 Gy (1.175 Gy/min).

Coculture of NIH/3T3 cells with MLE-12 cell supernatant

After continued culture for 48 hours after irradiation of MLE-12 cells, the supernatant of MLE-12 cells was collected by centrifugation. Then, the supernatant was co-cultured with NIH/3T3 cells for 72 hours. Myofibroblast markers were detected by western blot and quantitative polymerase chain reaction (qPCR).

RNA interference

Lipofectamine RNAiMAX were applied to transfections of small interfering RNA (siRNA) according to the manufacturer's protocol (Invitrogen, San Diego, USA). The siRNA sequence for STING was synthesized by GenePharma company (Shanghai, China). The siRNA sequence used in this study is shown in Table S1.

Western blot

The treated cells or tissues were lysed by RIPA solution, separated by sodium dodecyl sulphate-polyacrylamide gel electrophoresis (SDS-PAGE) and transferred to polyvinylidene fluoride (PVDF) membranes. Membranes were blocked with 5% skim milk for 1 hour, antibodies were incubated overnight at 4 ℃ and washed three times with Tris-Buffered Saline with Tween-20 (TBST), followed by secondary antibodies for 1 hour at room temperature. α-tubulin was used as an internal reference. Then the strips were visualized by chemiluminescence. Imaging was performed using the Tanon imaging system.

Reverse transcription quantitative polymerase chain reaction (RT-qPCR)

According to the manufacturer's instruction, total RNA was extracted from cells or tissues with TRIzol reagent (Invitrogen). RNA was dissolved in 40 μL RNase-free ddH_2O. Total RNA was quantified using Nanodrop instrument (Thermo Fisher Scientific) and stored at –80 ℃ for subsequent experiments. Then, complementary DNA (cDNA) synthesis was performed by using the HiScript III qRT SuperMix for qPCR (Vazyme). qPCR was performed using Taq Pro Universal SYBR qPCR Master Mix (Vazyme). The qPCR reaction was conducted on the Applied Biosystems 7500 Fast Real-Time PCR System (Thermo Fisher Scientific) for 40 cycles, following the manufacturer's protocol. The relative expression of targeted mRNA is calculated by $2^{-\Delta\Delta Ct}$ method. And β-actin is selected as endogenous control. Relevant primer sequences are shown in Table S2.

Measurement of dsDNA

dsDNA was measured in the BALF, serum and cell supernatant using dsDNA HS Assay Kit (Invitrogen), according to the manufacturer's protocol. After incubation at room temperature in the dark for 2 min, quantitative detection of dsDNA was performed using the Qubit fluorometer.

Cellular senescence assay

β-galactosidase staining kit (Beyotime) was used to detect cellular senescence according to the manufacturer's protocol. After the treated cells were fixed at room temperature for 15 min, the working solution was added and incubated at 37 ℃ overnight. Images were then acquired through an inverted microscope.

Statistical analysis

GraphPad Prism 8.0 and SPSS 25.0 were used for data analysis. The data were independently repeated for three times, and expressed as means ± standard deviation (SD). Analysis of variance (ANOVA) and Student's *t*-test were used to assess the statistical significance of the data. $P<0.05$ was considered statistically significant.

Results

Irradiation could activate cGAS-STING pathway, and early application of STING inhibitor H-151 protected mice from lung injury caused by radiation exposure

The animal models were established by a single 20 Gy whole-thorax irradiation of C57BL/6J mice. The dsDNA concentration was detected in serum and BALF after irradiation. We observed that dsDNA concentration in serum and BALF of mice after irradiation was significantly increased compared with the control group, with the most significant concentration at 12 hours (*Figure 1A*,*1B*). Western blot result showed that the expression levels of cGAS and STING proteins of lung tissues were significantly increased (*Figure 1C*). These results suggested that irradiation-induced lung injury may be closely related to the cGAS-STING pathway.

Subsequently, we established a mouse model of RILI (*Figure 1D*). Mice were exposed to a single 20 Gy whole-thorax irradiation. Beginning on the day of irradiation, the treatment group was given the STING inhibitor H-151 by intraperitoneal injection at a dose of 10.5 mg/kg for 4 weeks. Lung tissues and serum were collected at 1, 2, 4, 12 and 24 weeks after irradiation. As shown in the representative images of mice 12 weeks after irradiation (*Figure 1E*), compared with the control group, the irradiated group showed obvious hair loss and discoloration in the exposed area of the chest, while the irradiated mice treated with H-151 showed significant improvement in the chest hair. In addition, we calculated the lung coefficient (lung weight/body weight) of the mice, which served as an indicator of the extent of pulmonary edema or fibrosis. The lung coefficient of mice in the irradiation group was significantly higher than that in the control group, while the lung coefficient of mice in the early intervention group

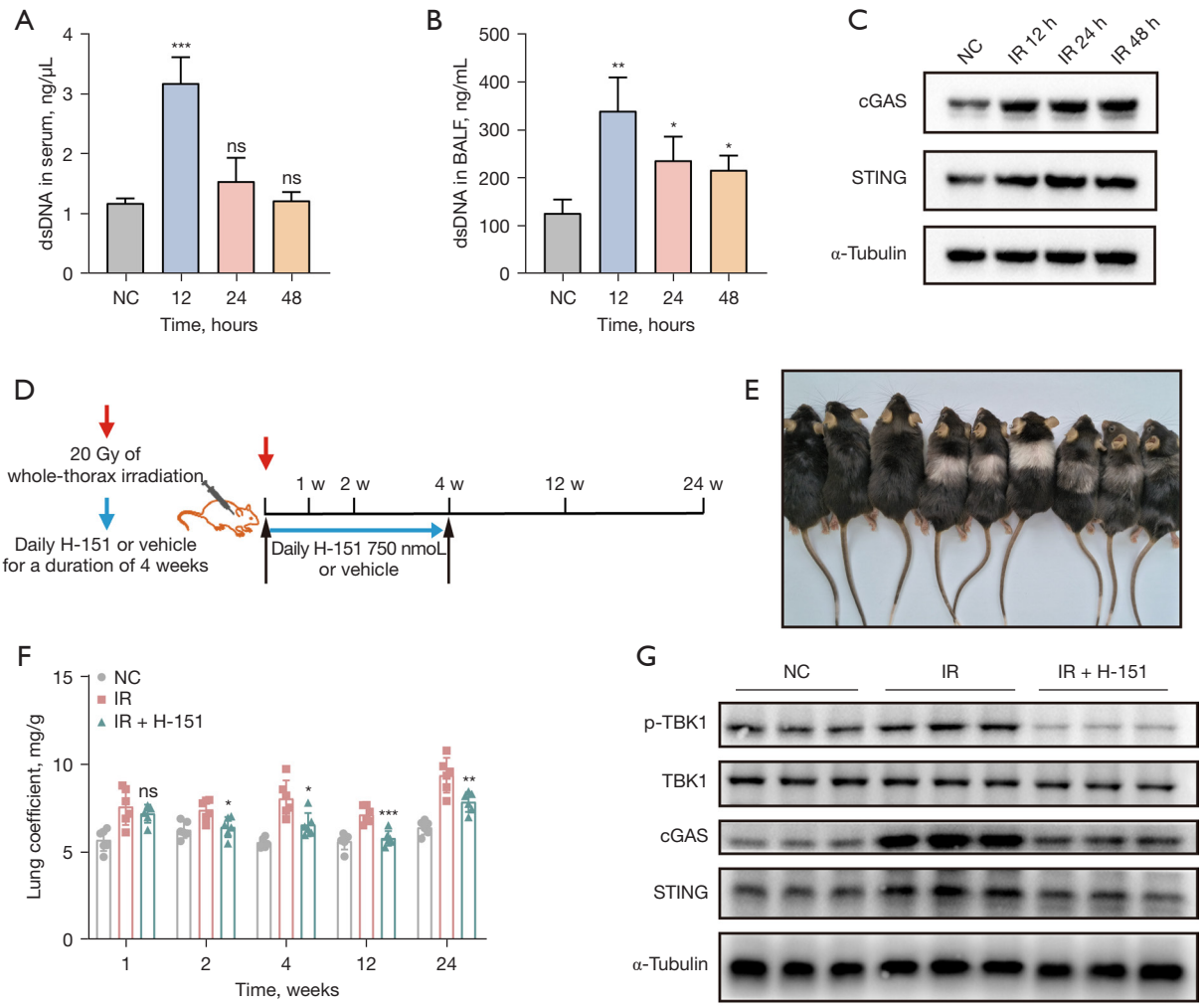

Figure 1 Early application of STING inhibitor H-151 protected mice from radiation-induced lung injury. The levels of dsDNA in serum (A) and BALF (B) were detected. (C) The expression of cGAS and STING protein was detected by western blot. (D) Schematic diagram of the establishment of a mouse model of RILI. (E) Representative images of mice at 12 weeks after irradiation. (F) Changes in lung coefficients after 20 Gy whole-thorax irradiation. (G) Western blot was used to detect the activation of cGAS-STING pathway in lung tissue. Data are shown as mean ± standard deviation of triplicate measurements; n=6. *, P<0.05; **, P<0.01; ***, P<0.001. dsDNA, double-stranded DNA; BALF, bronchoalveolar lavage fluid; cGAS, cyclic guanosine monophosphate-adenosine monophosphate synthase; STING, stimulator of interferon genes; NC, negative control; IR, irradiation; ns, not significant.

given STING inhibitor was significantly lower (*Figure 1F*). Taking the lung tissue 4 weeks after irradiation as an example, western blot results showed that the expression levels of cGAS, STING and p-TBK1 proteins were significantly increased after irradiation, while the expression levels of the above proteins were significantly decreased in the lung tissue of mice treated with H-151 (*Figure 1G*). In summary, irradiation could cause abnormal activation of cGAS-STING pathway, and early administration of STING inhibitor H-151 could effectively inhibit its activation.

H-151 alleviated the infiltration of lung inflammatory cells and reduced the expression of pro-inflammatory cytokines

H&E staining was used to observe the pathological changes of lung tissue. The results showed that the alveolar structure of the normal group was complete, the alveolar wall was thin and clearly visible, the capillaries were intact, and there

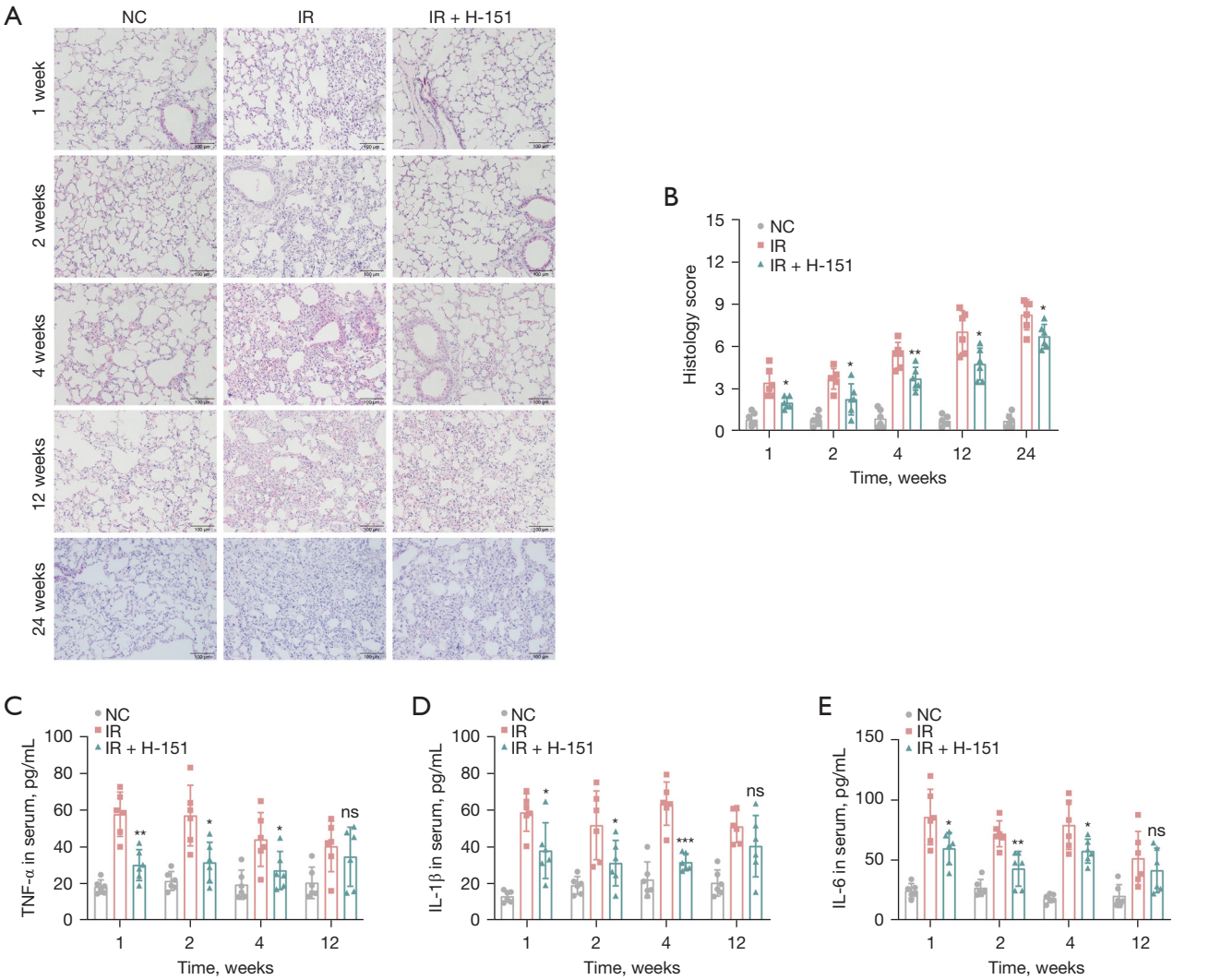

Figure 2 Early application of STING inhibitor H-151 alleviated the radiation pneumonitis in mice. (A) Representative images of H&E staining of lung tissue. Scale bar, 100 μm. (B) Histology scoring result of (A). The levels of inflammatory cytokines TNF-α (C), IL-1β (D) and IL-6 (E) in serum were detected by ELISA. Data are shown as mean ± standard deviation of triplicate measurements; n=6. *, P<0.05; **, P<0.01; ***, P<0.001. NC, negative control; IR, irradiation; TNF-α, tumor necrosis factor-alpha; IL, interleukin; ns, not significant; STING, stimulator of interferon genes; H&E, hematoxylin and eosin; ELISA, enzyme-linked immunosorbent assay.

was no obvious inflammatory cell seepage. The widening of alveolar wall and destruction of alveolar space were observed in the irradiation group, accompanied by thickening of lung texture and a large number of inflammatory cell infiltration, while the inflammatory cell infiltration was significantly reduced in the treatment group (*Figure 2A,2B*), suggesting that H-151 could significantly alleviate the acute lung injury caused by irradiation. Serum levels of representative pro-inflammatory cytokines, including TNF-α, IL-1β and IL-6, were measured by ELISA kits. These cytokines were significantly elevated under the influence of radiation, which were effectively decreased after treatment (*Figure 2C-2E*). Overall, early intervention with STING inhibitor H-151 significantly alleviated the severity of radiation pneumonia.

Early intervention of H-151 inhibited radiation-induced chronic pulmonary fibrosis

Next, we explored whether early administration of STING inhibitor H-151 could delay the progression of advanced

chronic pulmonary fibrosis after radiation. Masson staining showed that with the extension of time after irradiation, the lung pathology of mice in the irradiation group showed obvious collagen deposition, while the content of collagen in the treatment group significantly decreased, especially after 24 weeks (*Figure 3A,3B*). Immunohistochemical staining showed that the expression level of COL1A1 protein in lung tissue of mice was significantly increased after irradiation, while it was significantly decreased after STING inhibitor treatment (*Figure 3C,3D*). As we know, α-smooth muscle actin (α-SMA) is also a marker of fibrosis. Immunohistochemical staining and western blot results confirmed that α-SMA expression in the treatment group was significantly lower than that in the irradiation group at the later stage. The mRNA expression of α-SMA (Acta2) was consistent with the above results (*Figure 3E-3H*). These results suggested that early intervention with STING inhibitor could also significantly mitigate the progression of chronic radiation pulmonary fibrosis.

dsDNA derived from pulmonary epithelial cells promoted the transformation of fibroblasts into myofibroblasts

As we know, pulmonary epithelial cells are one of the main cell types involved in RILI (21). Fibrosis is characterized by the accumulation of myofibroblasts, which are mainly converted from fibroblasts. Therefore, we aimed to investigate whether irradiation would promote the transformation of fibroblasts into myofibroblasts through damaging pulmonary epithelial cells. Firstly, we irradiated the mouse pulmonary epithelial cell line MLE-12 with a dose of 10 Gy and measured the dsDNA content in the cell supernatant. The results showed that the dsDNA content in the supernatant of MLE-12 cell line significantly increased after irradiation, and this trend became more pronounced with prolonged time (*Figure 4A*). Furthermore, by comparing the difference in dsDNA content in the supernatant between pulmonary epithelial cell line MLE-12 and fibroblast cell line NIH/3T3 after 48 hours of irradiation, the results showed a significant increase in dsDNA released by MLE-12 cell line compared to NIH/3T3 cell line (*Figure 4B*), suggesting that pulmonary epithelial cells may be the primary target cells for radiation-induced injury.

Next, we irradiated the MLE-12 cell line with a dose of 10 Gy and collected the cell supernatant after 48-hour cultivation. The collected supernatant was co-cultured with NIH/3T3 cells for 72 hours. Western blot results showed the expression levels of α-SMA and Collagen I proteins in irradiated NIH/3T3 cell line were significantly increased. Regardless of whether NIH/3T3 cell line was irradiated or not, co-culturing them with epithelial cell supernatant significantly increase the expression level of the above proteins (*Figure 4C*). The results prompted that the supernatant of mouse pulmonary epithelial cells after irradiation could stimulate fibroblast-to-myofibroblast transformation. Furthermore, we speculated that dsDNA is the main supernatant component which responsible for the transformation.

Therefore, we added an artificial synthetic analogue of dsDNA [poly(dA:dT) at a concentration of 4 μg/mL]. Western blot results showed that the addition of poly(dA:dT) after irradiation significantly increased the expression levels of α-SMA and Collagen I protein in NIH/3T3 cell line (*Figure 4D*). What's more, we found that the mRNA expression levels of α-SMA, Fibronectin-1 and ZEB1 in the co-cultured group were significantly increased ($P<0.05$, *Figure 4E-4G*). Similarly, immunofluorescence also confirmed the significant upregulation of α-SMA expression after adding poly(dA:dT) (*Figure 4H*). These results suggested that the irradiation induces fibroblast-to-myofibroblast transformation, and exogenous dsDNA stimulation further enhances the effect.

In order to further clarify the key role of dsDNA in the supernatant, we added Dnase I (0.15 U/μL) for intervention. We found that the expression levels of α-SMA and Collagen I proteins were significantly decreased after Dnase I treatment (*Figure 5A*), and the mRNA levels of fibrosis markers such as α-SMA (Acta2), Fibronectin-1, ZEB1 were significantly down-regulated (*Figure 5B-5D*). Immunofluorescence assay confirmed that the expression of α-SMA protein in NIH/3T3 cells was significantly enhanced after the addition of the supernatant of irradiated MLE-12 cells, and decreased significantly after the addition of Dnase I (*Figure 5E*). These results suggested that the supernatant from irradiated mouse pulmonary epithelial cells could stimulate fibroblast-to-myofibroblast transformation, while the vital component in the supernatant was dsDNA released by the epithelial cells.

STING mediated the activation of fibroblasts to myofibroblasts via the PERK-eIF2α pathway

A previous study (22) reported that inhibition of STING could block pathological activation of cardiac fibroblasts. Now that pulmonary epithelial cells-derived dsDNA can stimulate fibroblast-to-myofibroblast transformation, we

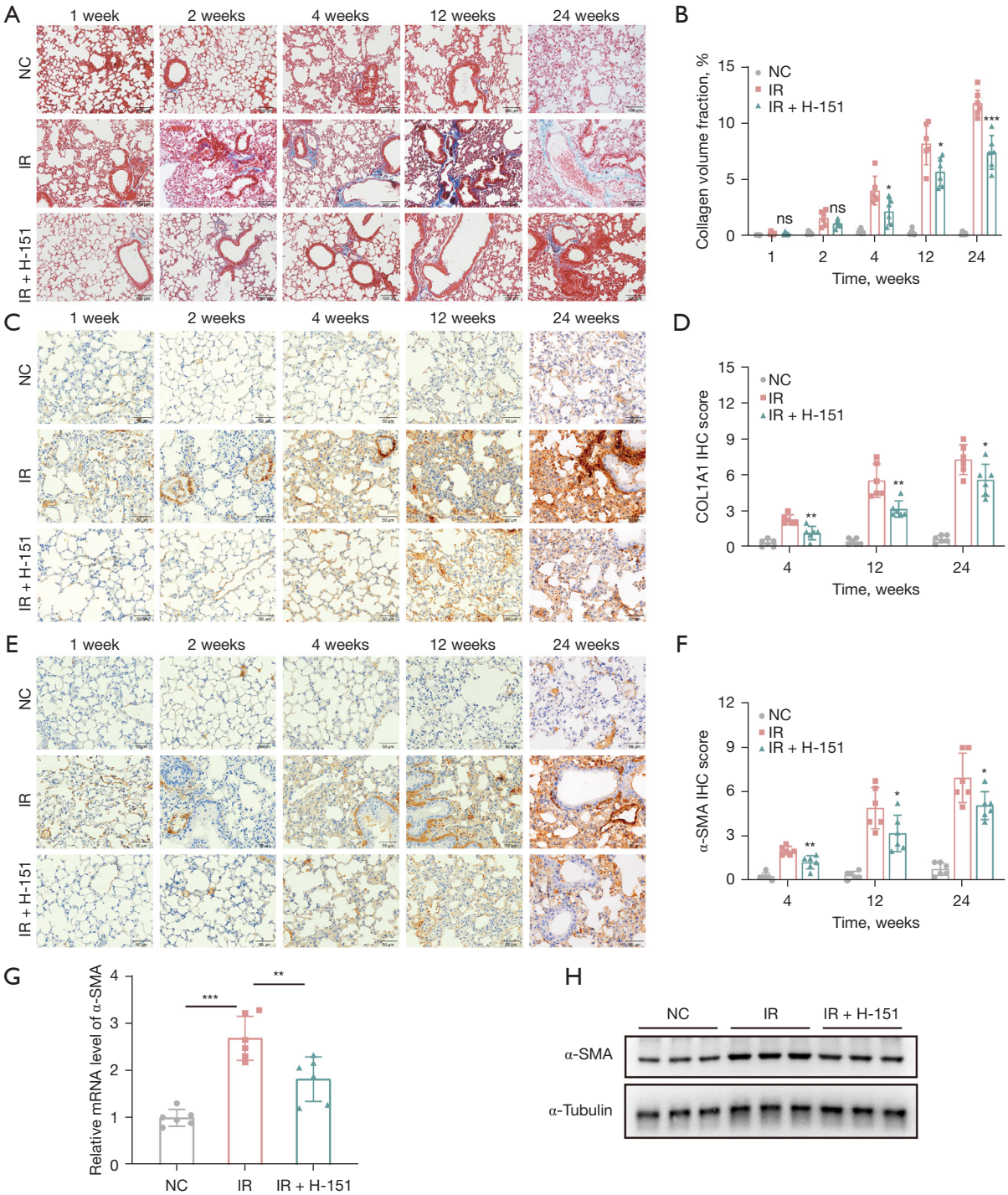

Figure 3 H-151 ameliorated radiation-induced pulmonary fibrosis in mice. (A) Representative images of Masson staining of lung tissue. Scale bar, 100 μm. (B) Quantitative statistical results of (A). (C) Representative images of immunohistochemical staining of COL1A1. Scale bar, 50 μm. (D) Quantitative statistical results of (C). (E) Representative images of immunohistochemical staining of α-SMA. Scale bar, 50 μm. (F) Quantitative statistical results of (E). (G) Relative mRNA level of α-SMA was detected by RT-qPCR. (H) The protein expression level of α-SMA was detected by western blot. Data are shown as mean ± standard deviation of triplicate measurements; n=6. *, P<0.05; **, P<0.01; ***, P<0.001. NC, negative control; IR, irradiation; IHC, immunohistochemistry; RT-qPCR, reverse transcription quantitative polymerase chain reaction.

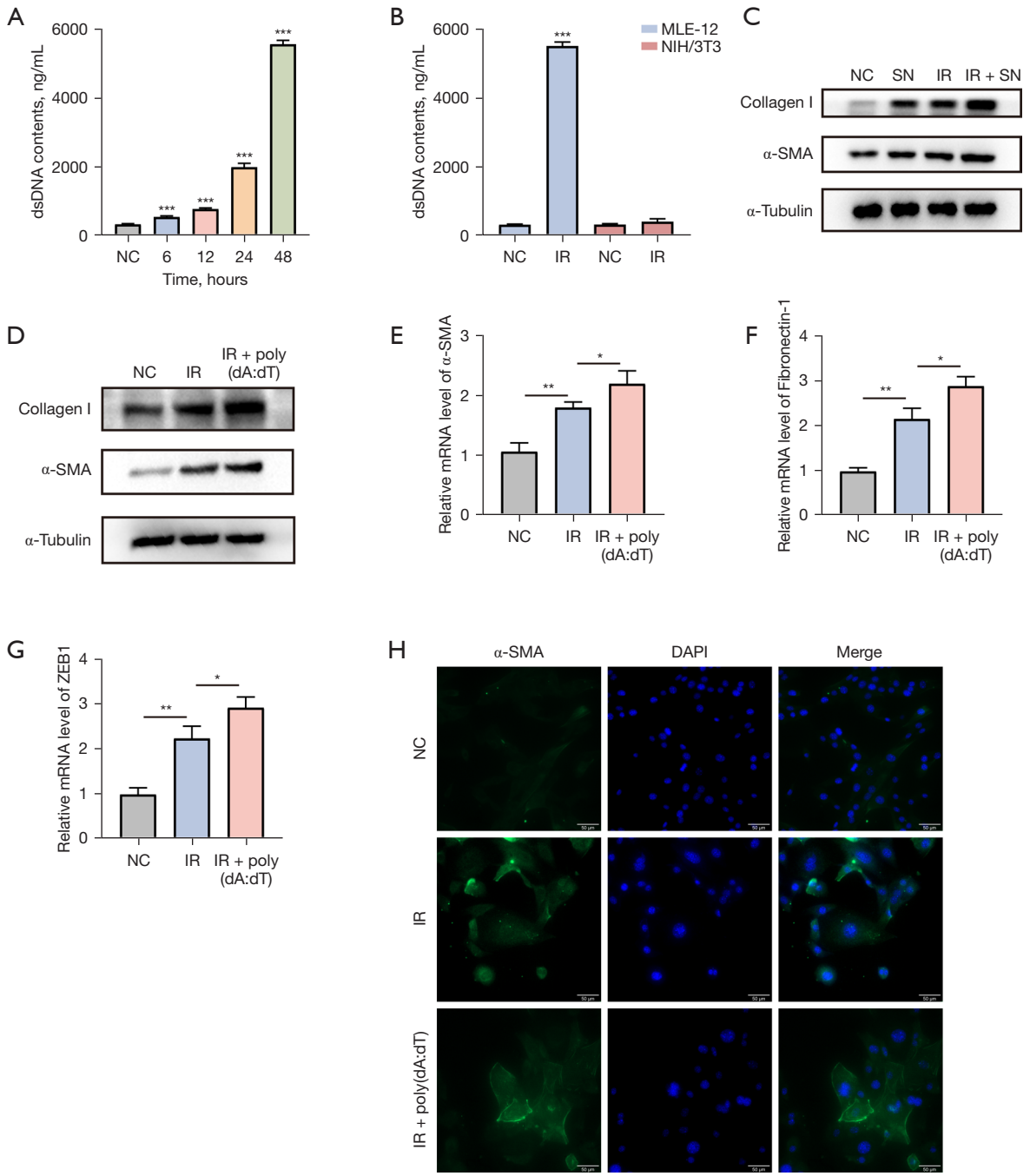

Figure 4 dsDNA derived from pulmonary epithelial cells promoted the transformation of fibroblasts into myofibroblasts. (A) dsDNA content in the supernatant of irradiated MLE-12 cells was detected. (B) Comparison of the dsDNA content between the supernatants of MLE-12 cells and NIH/3T3 cells. (C) After NIH/3T3 cells were co-cultured with the MLE-12 cells' supernatant, the expression levels of α-SMA and Collagen I in NIH/3T3 cells were detected. (D) The protein expression levels of α-SMA and Collagen I in NIH/3T3 cells after adding poly(dA:dT) were detected by western blot. The mRNA expression levels of fibrosis-related factors α-SMA (E), Fibronectin-1 (F), and ZEB1 (G) were measured by RT-qPCR after the addition of poly(dA:dT). (H) The expression level of α-SMA in NIH/3T3 cells after adding poly(dA:dT) was detected by immunofluorescence. Scale bar, 50 μm. Data are shown as mean ± standard deviation of triplicate measurements; n=6. *, P<0.05; **, P<0.01; ***, P<0.001. dsDNA, double-stranded DNA; NC, negative control; IR, irradiation; SN, supernatant; DAPI, 4',6-diamidino-2-phenylindole; RT-qPCR, reverse transcription quantitative polymerase chain reaction.

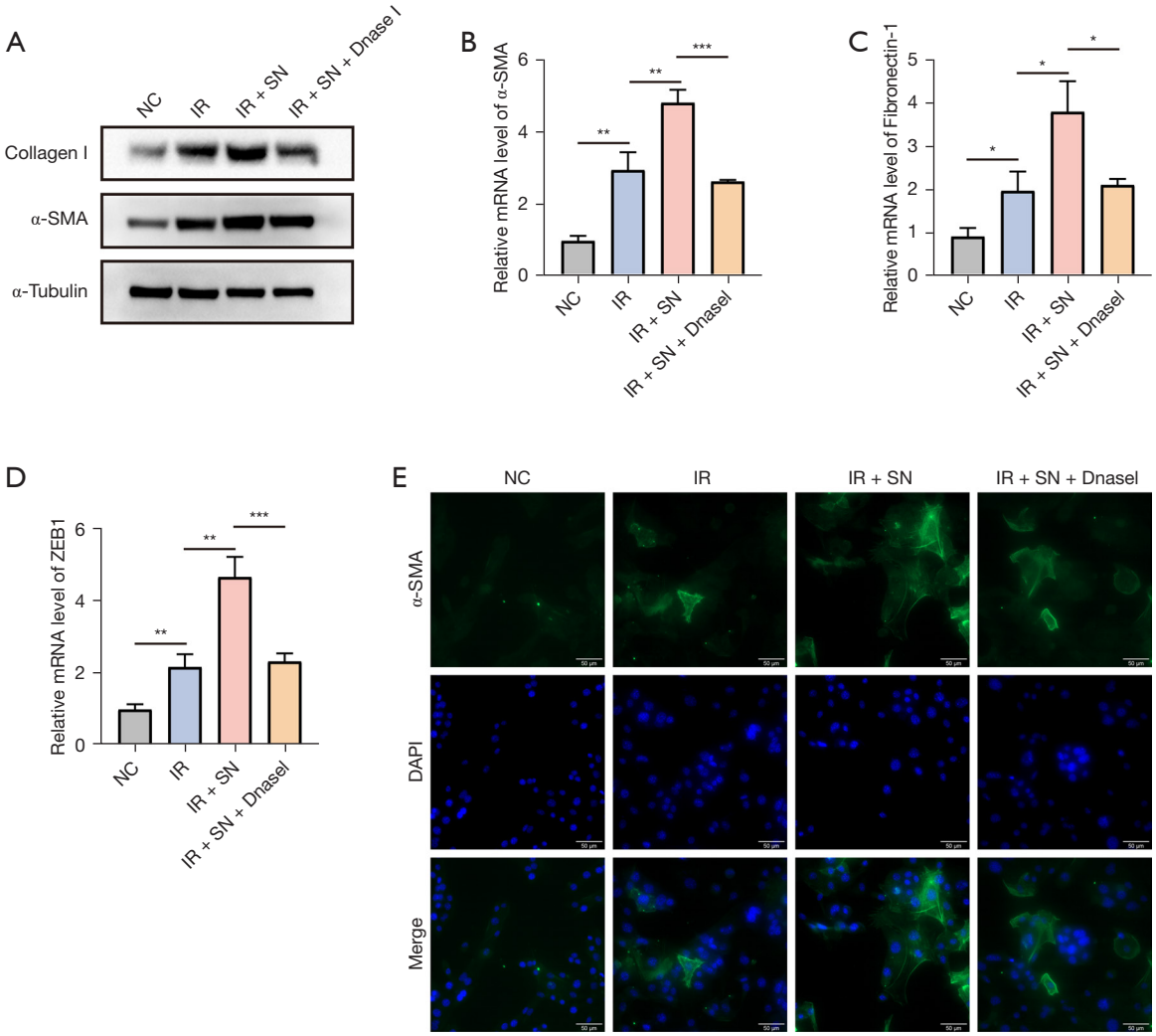

Figure 5 Dnase I effectively interfered with the transformation of fibroblasts into myofibroblasts caused by supernatant. (A) The protein expression levels of α-SMA and collagen I in NIH/3T3 cells after adding Dnase I were detected by western blot. The mRNA expression levels of fibrosis-related factors α-SMA (B), Fibronectin-1 (C), and ZEB1 (D) were measured by RT-qPCR after the addition of Dnase I. (E) The expression level of α-SMA in NIH/3T3 cells after adding Dnase I was detected by immunofluorescence. Scale bar, 50 μm. Data are shown as mean ± standard deviation of triplicate measurements; n=6. *, P<0.05; **, P<0.01; ***, P<0.001. RT-qPCR, reverse transcription quantitative polymerase chain reaction; DAPI, 4',6-diamidino-2-phenylindole; NC, negative control; IR, irradiation; SN, supernatant.

investigated whether STING mediates this regulatory process. Western blot found that the expression of α-SMA protein in NIH/3T3 cell was significantly up-regulated after adding the supernatant of irradiated MLE-12 cell line. However, knockdown of STING significantly reversed this process (*Figure 6A*). Similarly, the mRNA levels of fibrosis markers such as α-SMA, Fibronectin-1, and ZEB1 were no longer significantly increased in NIH/3T3 cells after knockdown of STING followed by addition of irradiated MLE-12 cell supernatant (*Figure 6B-6D*). Overall, STING could mediate the activation of epithelial-derived dsDNA for fibroblast transformation.

A recent study demonstrated that the STING-PERK-eIF2α pathway plays a vital role in cellular senescence and organ fibrosis (18). However, it is still unclear whether the STING-PERK pathway regulates fibroblast behavior during RILI. The results confirmed that the phosphorylation levels of PERK and eIF2α increased with the addition of supernatant, while decreased significantly after STING knockdown (*Figure 6E*), suggesting that

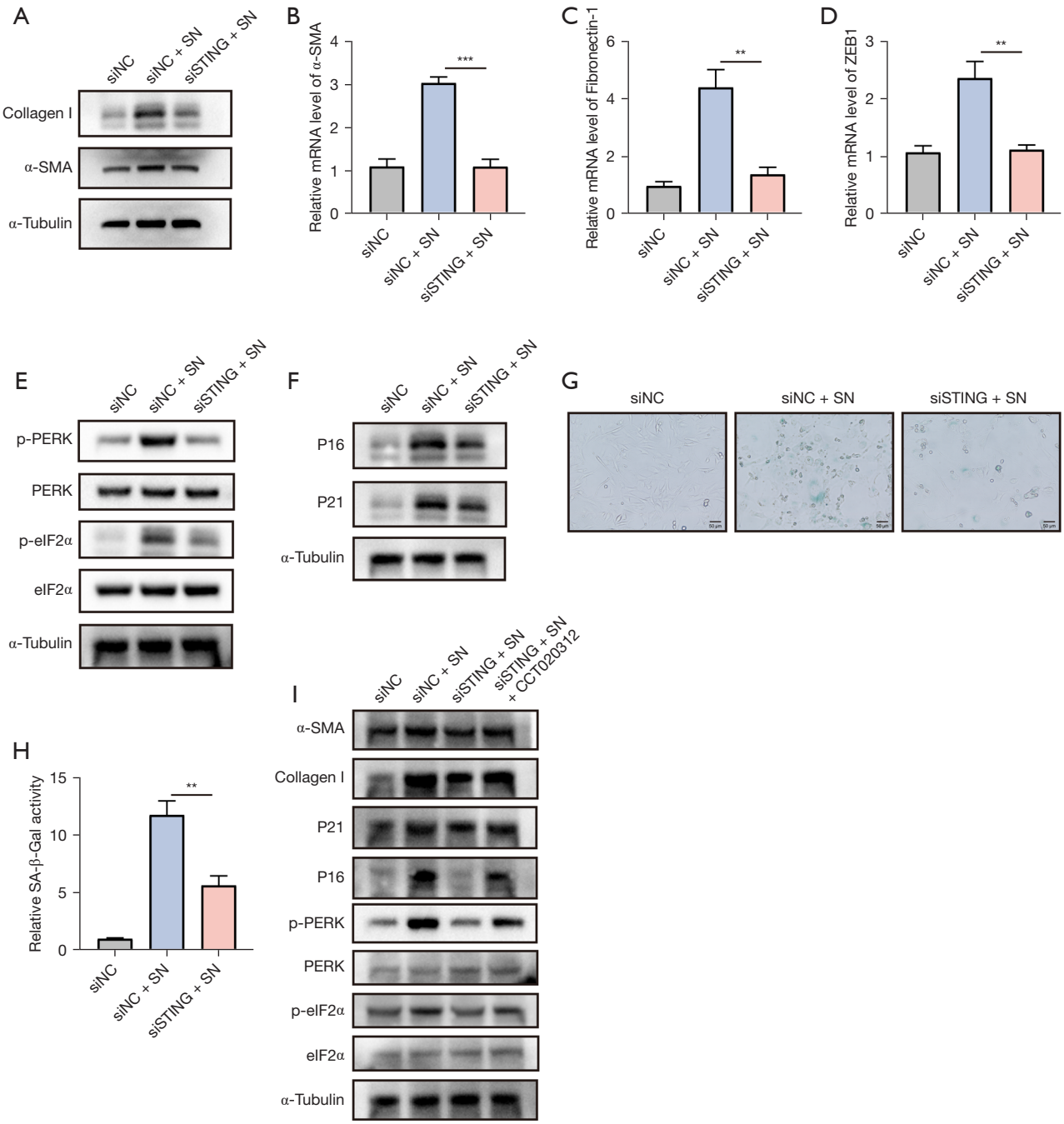

Figure 6 STING mediated the activation of fibroblasts to myofibroblasts via the PERK-eIF2α pathway. (A) The protein expression levels of α-SMA and Collagen I were detected by western blot after STING knockdown. The mRNA expression levels of fibrosis-related factors α-SMA (B), Fibronectin-1 (C) and ZEB1 (D) were measured by RT-qPCR. (E) The protein expression levels of PERK-eIF2α pathway were determined by western blot analysis. (F) The protein expression levels of P16 and P21 were determined by western blot. (G) Cellular senescence was assessed by SA-β-Gal staining. (H) Quantitative statistical results of (G). (I) STING mediates fibroblast to myofibroblast activation via PERK-eIF2α pathway, which was confirmed by western blot. Scale bar, 50 μm. Data are shown as mean ± standard deviation of triplicate measurements. **, P<0.01; ***, P<0.001. NC, negative control; SN, supernatant; PERK, PKR-like endoplasmic reticulum kinase; eIF2α, eukaryotic initiation factor 2α; STING, stimulator of interferon genes; RT-qPCR, quantitative reverse transcription polymerase chain reaction.

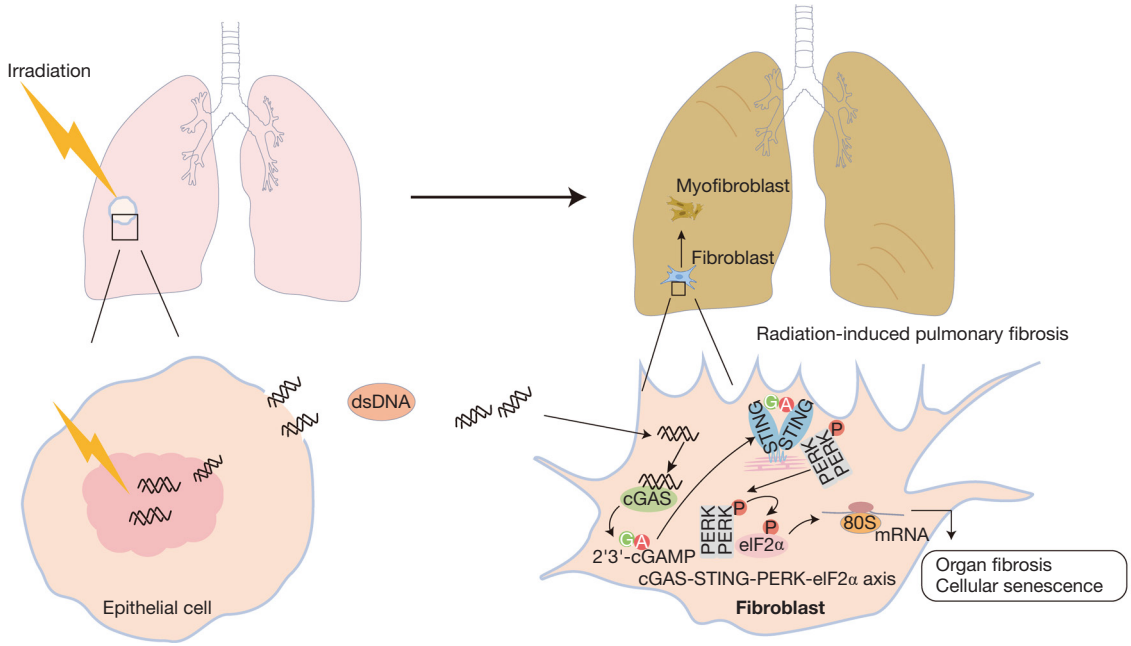

Figure 7 A graphic illustration of the mechanism of STING-mediated radiation-induced lung injury. dsDNA, double-stranded DNA; cGAS, cyclic guanosine monophosphate-adenosine monophosphate synthase; STING, stimulator of interferon genes; PERK, PKR-like endoplasmic reticulum kinase; eIF2α, eukaryotic initiation factor 2α; cGAMP, cyclic guanosine monophosphate-adenosine monophosphate.

STING could mediate the stimulation of the PERK-eIF2α pathway by supernatant. Meanwhile, we also verified the effect of supernatant on fibroblast senescence. The increased expression of P16 and P21 induced by supernatant was significantly interfered with by STING knockdown (*Figure 6F*). And the β-galactosidase staining also confirmed the above conclusion (*Figure 6G,6H*). We then further verified whether STING mediated myofibroblast transformation through PERK-eIF2α pathway. We found that the PERK activator CCT020312 could activate the PERK-eIF2α pathway and then significantly increase the protein levels of α-SMA and Collagen I (*Figure 6I*). Overall, these results suggested that STING could mediate fibroblast-to-myofibroblast transformation through PERK-eIF2α pathway (*Figure 7*).

Discussion

RILI is one of the common radiotherapy-related complications, mainly manifested as cough, shortness of breath, chest pain and other symptoms (23). In a few hours to a few days after lung irradiation, acute inflammation is dominant, early radiation pneumonia can be controlled by drugs (24). As a late complication, radiation-induced pulmonary fibrosis is often irreversible once it occurs, with a high mortality rate due to the lack of effective drug treatment (25). RILI is the main dose-limiting factor affecting the effect of radiotherapy, which not only affects the treatment and prognosis of patients, but also causes respiratory failure and even death in severe cases (26).

The pathophysiological process of RILI includes early inflammatory response and late fibrosis process (27). RILI is a continuous progressive process observed from the molecular level (28). Irradiation of lung tissue can cause dsDNA cleavage of cells and produce a large amount of reactive oxygen species, which can cause damage and apoptosis of alveolar epithelial cells and vascular endothelial cells (29,30). At the same time, it is accompanied by the infiltration of inflammatory cells and the secretion of pro-inflammatory factors (31). To explore the relationship between dsDNA and lung inflammation, our study showed that irradiation could cause an abnormal elevation of dsDNA in serum and alveolar lavage fluid in mice. dsDNA has been reported as an upstream stimulus of the cGAS-STING pathway. Further, the expression levels of cGAS and STING proteins in lung tissue were significantly increased, which suggests that RILI may be closely related to the cGAS-STING pathway. Early application of STING

inhibitor H-151 could reduce the excessive production of pro-inflammatory factors TNF-α, IL-6 and IL-1β in the serum of mice induced by irradiation, and inhibit the infiltration of inflammatory cells. Our study demonstrated that STING was involved in the radiation-induced inflammatory response of the lung.

The body's inflammatory response is a double-edged sword. The occurrence of early inflammatory response is the necessary defense mechanism of the body, while excessive inflammation will induce body damage and pathological fibrosis (27). To further evaluate the protective effect of H-151 on RIPF, our study examined collagen deposition and α-SMA expression level in lung tissue by Masson staining, immunohistochemical staining, RT-qPCR and western blot. The results showed that early application of H-151 significantly reduced irradiation-induced collagen deposition and α-SMA expression level, suggesting that STING restriction can reduce the severity of RIPF. Besides regulating IRF3 signaling after phosphorylation of TBK1, cGAS-STING pathway also activates PERK/eIF2α pathway, which leads to senescence, fibrosis and other cellular processes (32,33). However, it has not been reported whether the cGAS-STING pathway regulates fibroblast behavior during RIPF.

The transformation of fibroblasts into myofibroblasts is the core link of RIPF (34). Myofibroblasts can produce a large number of extracellular matrix (ECM) adhesive and structural proteins, which are marked by the expression of α-SMA (35). Previous studies have found that the recruitment and transformation of fibroblasts is a complex process, in which endothelial cells, macrophages and others are involved in its regulation (36,37). In our study, we found that irradiation of the lung epithelial cell line MLE-12 with a dose of 10 Gy resulted in a significant increase of dsDNA content in its cell supernatant. Meanwhile, dsDNA derived from epithelial cells significantly increased the expression level of α-SMA in NIH/3T3 cells. And the mRNA levels of fibrosis-related factors α-SMA, ZEB1 and Fibronectin-1 also significantly increased. The results were further confirmed by using synthetic dsDNA [poly(dA:dT)] and Dnase I. Finally, knockdown of STING reversed the degree of myofibroblast transformation by inhibiting the PERK-eIF2α pathway, which suggests that STING plays a key role in the regulation of RIPF.

However, there are some limitations in this study. Firstly, while our current results strongly support the therapeutic promise of STING inhibition in RILI using mouse models and cellular studies, we recognize the importance of translating these findings into clinical settings. Therefore, it is highly necessary to conduct research with human cell lines, especially human fibroblasts, to further enhance the underlying mechanisms of STING inhibitors in RILI. Secondly, activation of the cGAS-STING pathway is pivotal in inducing an anti-tumor immune response. It is necessary to ensure that STING inhibitors can effectively treat RILI without interfering with the radiotherapy effect and the anti-tumor immune response. Specifically, we have elaborated on the potential clinical applications of STING inhibitors in the context of RILI in lung cancer patients, highlighting the need for rigorous preclinical and clinical investigations to optimize their use and ensure their safety and efficacy. Finally, traditional radiotherapy and modern radiotherapy such as stereotactic body radiation therapy (SBRT) may have different effects on normal cells due to different modes of action. Therefore, it is worth further investigation whether the STING inhibitor, as a potential therapeutic strategy for RILI, should be adjusted or implemented more accurately based on different radiotherapy modes.

Conclusions

Overall, our study focuses on the activation of cGAS-STING signaling pathway in RILI, and inhibition of STING significantly ameliorated RILI in mice. On the one hand, we found that STING mediated the effect of radiation-induced dsDNA release to stimulate the activation of inflammatory response. On the other hand, dsDNA released from irradiated lung epithelial cells could activate the transformation of fibroblasts into myofibroblasts, and STING restriction significantly delayed the fibrosis process through PERK-eIF2α pathway. The study demonstrated the protective effect of STING inhibitor on RILI and provided new insights into the underlying molecular mechanism and treatment of RILI.

Acknowledgments

The authors thank all staff in the Laboratory Animal Centre of the Beijing Institute of Radiation Medicine for their support during this study.
Funding: None.

Footnote

Reporting Checklist: The authors have completed the ARRIVE reporting checklist. Available at https://tlcr.

amegroups.com/article/view/10.21037/tlcr-24-649/rc

Data Sharing Statement: Available at https://tlcr.amegroups.com/article/view/10.21037/tlcr-24-649/dss

Peer Review File: Available at https://tlcr.amegroups.com/article/view/10.21037/tlcr-24-649/prf

Conflicts of Interest: All authors have completed the ICMJE uniform disclosure form (available at https://tlcr.amegroups.com/article/view/10.21037/tlcr-24-649/coif). The authors have no conflicts of interest to declare.

Ethical Statement: The authors are accountable for all aspects of the work in ensuring that questions related to the accuracy or integrity of any part of the work are appropriately investigated and resolved. Experiments were performed under a project license (No. IACUC-DWZX-2022-864) approved by the Institutional Animal Care and Use Committee of the Beijing Institute of Radiation Medicine, in compliance with the Chinese national or institutional guidelines for the care and use of animals.

References

1. Ni J, Wang X, Wu L, et al. Sintilimab in combination with stereotactic body radiotherapy and granulocyte-macrophage colony-stimulating factor in metastatic non-small cell lung cancer: The multicenter SWORD phase 2 trial. Nat Commun 2024;15:7242.
2. Williams LJ, Kunkler IH, Taylor KJ, et al. Postoperative radiotherapy in women with early operable breast cancer (Scottish Breast Conservation Trial): 30-year update of a randomised, controlled, phase 3 trial. Lancet Oncol 2024;25:1213-21.
3. Boutry C, Moreau NN, Jaudet C, et al. Machine learning and deep learning prediction of patient specific quality assurance in breast IMRT radiotherapy plans using Halcyon specific complexity indices. Radiother Oncol 2024;200:110483.
4. Yan Y, Fu J, Kowalchuk RO, et al. Exploration of radiation-induced lung injury, from mechanism to treatment: a narrative review. Transl Lung Cancer Res 2022;11:307-22.
5. Zhu J, Ao X, Liu Y, et al. TNKS1BP1 mediates AECII senescence and radiation induced lung injury through suppressing EEF2 degradation. Respir Res 2024;25:299.
6. Chen YY, Wang M, Zuo CY, et al. Nrf-2 as a novel target in radiation induced lung injury. Heliyon 2024;10:e29492.
7. Voruganti Maddali IS, Cunningham C, McLeod L, et al. Optimal management of radiation pneumonitis: Findings of an international Delphi consensus study. Lung Cancer 2024;192:107822.
8. Kuipers ME, van Doorn-Wink KCJ, Hiemstra PS, et al. Predicting Radiation-Induced Lung Injury in Patients With Lung Cancer: Challenges and Opportunities. Int J Radiat Oncol Biol Phys 2024;118:639-49.
9. Gao D, Li T, Li XD, et al. Activation of cyclic GMP-AMP synthase by self-DNA causes autoimmune diseases. Proc Natl Acad Sci U S A 2015;112:E5699-705.
10. Dvorkin S, Cambier S, Volkman HE, et al. New frontiers in the cGAS-STING intracellular DNA-sensing pathway. Immunity 2024;57:718-30.
11. Chen Q, Sun L, Chen ZJ. Regulation and function of the cGAS-STING pathway of cytosolic DNA sensing. Nat Immunol 2016;17:1142-9.
12. Liu Y, Lu X, Qin N, et al. STING, a promising target for small molecular immune modulator: A review. Eur J Med Chem 2021;211:113113.
13. Zhang C, Shang G, Gui X, et al. Structural basis of STING binding with and phosphorylation by TBK1. Nature 2019;567:394-8.
14. Ishikawa H, Ma Z, Barber GN. STING regulates intracellular DNA-mediated, type I interferon-dependent innate immunity. Nature 2009;461:788-92.
15. Runde AP, Mack R, S J PB, et al. The role of TBK1 in cancer pathogenesis and anticancer immunity. J Exp Clin Cancer Res 2022;41:135.
16. Hu S, Gao Y, Gao R, et al. The selective STING inhibitor H-151 preserves myocardial function and ameliorates cardiac fibrosis in murine myocardial infarction. Int Immunopharmacol 2022;107:108658.
17. Du S, Chen G, Yuan B, et al. DNA sensing and associated type 1 interferon signaling contributes to progression of radiation-induced liver injury. Cell Mol Immunol 2021;18:1718-28.

18. Zhang D, Liu Y, Zhu Y, et al. A non-canonical cGAS-STING-PERK pathway facilitates the translational program critical for senescence and organ fibrosis. Nat Cell Biol 2022;24:766-82.
19. Garcia AN, Casanova NG, Valera DG, et al. Involvement of eNAMPT/TLR4 signaling in murine radiation pneumonitis: protection by eNAMPT neutralization. Transl Res 2022;239:44-57.
20. Haag SM, Gulen MF, Reymond L, et al. Targeting STING with covalent small-molecule inhibitors. Nature 2018;559:269-73.
21. Rao X, Zhou D, Deng H, et al. Activation of NLRP3 inflammasome in lung epithelial cells triggers radiation-induced lung injury. Respir Res 2023;24:25.
22. Zhang C, Hao H, Wang Y, et al. Intercellular mitochondrial component transfer triggers ischemic cardiac fibrosis. Sci Bull (Beijing) 2023;68:1784-99.
23. De Bruycker A, Schneiders F, Gulstene S, et al. Evaluation of chest CT-scans following lung stereotactic ablative radiotherapy: Challenges and new insights. Lung Cancer 2024;193:107848.
24. Yan Y, Zhu Y, Yang S, et al. Clinical predictors of severe radiation pneumonitis in patients undergoing thoracic radiotherapy for lung cancer. Transl Lung Cancer Res 2024;13:1069-83.
25. Zhang T, Mi J, Qin X, et al. Rosmarinic Acid Alleviates Radiation-Induced Pulmonary Fibrosis by Downregulating the tRNA N7-Methylguanosine Modification-Regulated Fibroblast-to-Myofibroblast Transition Through the Exosome Pathway. J Inflamm Res 2024;17:5567-86.
26. Hanania AN, Mainwaring W, Ghebre YT, et al. Radiation-Induced Lung Injury: Assessment and Management. Chest 2019;156:150-62.
27. Gao J, Peng S, Shan X, et al. Inhibition of AIM2 inflammasome-mediated pyroptosis by Andrographolide contributes to amelioration of radiation-induced lung inflammation and fibrosis. Cell Death Dis 2019;10:957.
28. Zheng J, Wang Y, Wang Z, et al. Near-infrared Nrf2 activator IR-61 dye alleviates radiation-induced lung injury. Free Radic Res 2022;56:411-26.
29. Santivasi WL, Xia F. Ionizing radiation-induced DNA damage, response, and repair. Antioxid Redox Signal 2014;21:251-9.
30. Tan J, Sun X, Zhao H, et al. Double-strand DNA break repair: molecular mechanisms and therapeutic targets. MedComm (2020) 2023;4:e388.
31. Liu X, Shao C, Fu J. Promising Biomarkers of Radiation-Induced Lung Injury: A Review. Biomedicines 2021;9:1181.
32. Zhou R, Ma Y, Tao Z, et al. Melatonin Inhibits Glucose-Induced Apoptosis in Osteoblastic Cell Line Through PERK-eIF2α-ATF4 Pathway. Front Pharmacol 2020;11:602307.
33. Jiao P, Fan W, Ma X, et al. SARS-CoV-2 nonstructural protein 6 triggers endoplasmic reticulum stress-induced autophagy to degrade STING1. Autophagy 2023;19:3113-31.
34. Maharaj S, Shimbori C, Kolb M. Fibrocytes in pulmonary fibrosis: a brief synopsis. Eur Respir Rev 2013;22:552-7.
35. Shinde AV, Humeres C, Frangogiannis NG. The role of α-smooth muscle actin in fibroblast-mediated matrix contraction and remodeling. Biochim Biophys Acta Mol Basis Dis 2017;1863:298-309.
36. Su L, Dong Y, Wang Y, et al. Potential role of senescent macrophages in radiation-induced pulmonary fibrosis. Cell Death Dis 2021;12:527.
37. Xiong S, Guo R, Yang Z, et al. Treg depletion attenuates irradiation-induced pulmonary fibrosis by reducing fibrocyte accumulation, inducing Th17 response, and shifting IFN-γ, IL-12/IL-4, IL-5 balance. Immunobiology 2015;220:1284-91.

Cite this article as: Ge X, Liu Q, Fan H, Yu H, Li J, Li Y, Qin B, Ma J, Wang J, Hu Y. STING facilitates the development of radiation-induced lung injury via regulating the PERK/eIF2α pathway. Transl Lung Cancer Res 2024;13(11):3010-3025. doi: 10.21037/tlcr-24-649

